PDGFRA, PDGFRB, EGFR, and downstream signaling activation in malignant peripheral nerve sheath tumor

Federica Perrone, Luca Da Riva, Marta Orsenigo, Marco Losa, Genny Jocollè, Clara Millefanti, Elisa Pastore, Alessandro Gronchi, Marco Alessandro Pierotti, and Silvana Pilotti

Experimental Molecular Pathology, Department of Pathology (F.P., L.D.R., M.O., M.L., G.J., C.M., E.P., S.P.), Department of Medical and Surgical Oncology (A.G.), and Scientific Management (M.A.P.), Fondazione IRCCS Istituto Nazionale dei Tumori, Milan, Italy

We investigated the activation of platelet-derived growth factor (PDGF) receptor A (PDGFRA), PDGF receptor B (PDGFRB), epidermal growth factor receptor (EGFR), and their downstream pathways in malignant peripheral nerve sheath tumors (MPNSTs). PDGFRA, PDGFRB, and EGFR were immunohistochemically, biochemically, cytogenetically, and mutationally analyzed along with the detection of their cognate ligands in 16 neurofibromatosis type 1 (NF1)-related and 11 sporadic MPNSTs. The activation of the downstream receptor pathways was also studied by means of v-akt murine thymoma viral oncogene homolog (AKT), extracellular signal-regulated kinase (ERK), and mammalian target of rapamycin (mTOR) Western blotting experiments, as well as rat sarcoma viral oncogene homolog (*RAS*), v-raf murine sarcoma viral oncogene homolog B1 (*BRAF*), phosphoinositide-3-kinase, catalytic, alpha polypeptide (*PI3KCA*), and phosphatase and tensin homolog deleted on chromosome ten (*PTEN*) mutational analysis and fluorescence in situ hybridization. PDGFRA, PDGFRB, and EGFR were expressed/activated, with higher levels of EGFR expression/phosphorylation paralleling increasing *EGFR* gene copy numbers in the NF1-related cases (71%). Autocrine loop activation of these receptors along with their coactivation were suggested by the expression of the cognate ligands in the absence of mutations and the presence of receptor tyrosine kinase (RTK) heterodimers, respectively. Both MPNST groups showed AKT, ERK, and mTOR expression/phosphorylation. No *BRAF*, *PI3KCA*, or *PTEN* mutations were found in either group of MPNSTs, but 18% of the sporadic MPNSTs showed *RAS* mutations. *PTEN* monosomy segregated with the NF1-related cases (50%, $p = 0.018$), but PTEN protein was expressed in all but two cases. In conclusion, PDGFRA, PDGFRB, and EGFR seem to be promising molecular targets for tailored treatments in MPNST. In particular, the ligand- and heterodimerization-dependent RTK activation/expression coupled with a downstream signaling phosphorylation, mediated by the upstream receptors or RAS activation, may provide a rationale to apply combined RTK and mTOR inhibitor treatments both to sporadic and NF1-related cases.
Neuro-Oncology 11, 725–736, 2009 (Posted to Neuro-Oncology [serial online], Doc. D08-00224, February 26, 2009. URL http://neuro-oncology.dukejournals.org; DOI: 10.1215/15228517-2009-003)

Keywords: EGFR, MPNST, mTOR, PDGFRA, PDGFRB

Malignant peripheral nerve sheath tumors (MPNSTs) are rare aggressive soft tissue neoplasms characterized by a poor prognosis that can arise sporadically or in association with neurofibromatosis type 1 (NF1), a hereditary tumor syndrome.[1] Surgery is the only effective therapeutic approach

Received August 26, 2008; accepted December 24, 2008.

Address correspondence to Silvana Pilotti, Department of Pathology, Fondazione IRCCS Istituto Nazionale dei Tumori, Via Venezian, 1, 20133 Milan, Italy (silvana.pilotti@istitutotumori.mi.it).

because chemo- and radiotherapy do not seem to lead to significant results.

A number of molecular and genetic alterations have been found in relation to these tumors, such as mutations in the tumor protein p53 (TP53) gene,[2,3] which are mainly restricted to sporadic MPNSTs,[4,5] and the loss of chromosome regions 17q, 17p, and 22q, which respectively encode *NF1*, *TP53*, and *NF2*.[4,6,7] Another particular hallmark of the genetic profile of both sporadic and NF1-related MPNSTs is the inactivation of the 9p21 locus, which harbors a gene cluster consisting of three tumor suppressor genes $p15^{INK4b}$, $p14^{ARF}$, and $p16^{INK4a}$.[8–10] This inactivation is mainly due to a homozygous deletion (less frequently promoter methylation)[8] and is coupled with the inactivation of the TP53 and retinoblastoma (Rb) pathways, which leads to severe consequences on cell growth control and apoptosis.

It has recently been shown that MPNSTs have molecular aberrations of receptor tyrosine kinase (RTK) genes: *KIT* and platelet-derived growth factor (PDGF) receptor A (*PDGFRA*) gene amplification and *PDGFRA* point mutations have been described in NF1-related cases,[11] which also obviously show *NF1* deletion and consequent RAS upregulation;[12] both NF1-associated and sporadic MPNSTs have been reported to express high levels of PDGFRA and its ligand, thus strongly suggesting an autocrine loop,[11] and high levels of PDGF receptor B (*PDGFRB*) mRNA and protein have been described in the absence of gene mutation.[13] Furthermore, it has been demonstrated that imatinib treatment suppresses the invasive activity and growth of MPNST cell lines by inhibiting PDGFA-ligand–induced PDGFRA phosphorylation[11] and PDGFB-ligand–induced PDGFRB phosphorylation.[13] All of these findings support the idea that PDGFRA and PDGFRB can be considered candidates for the targeted treatment of both sporadic and syndromic MPNSTs.

Finally, it has been reported that NF1-related and sporadic MPNSTs express epidermal growth factor receptor (EGFR) mRNA and protein,[13,14] and also show gene amplification,[15] thus suggesting that EGFR alterations may be involved in MPNST tumorigenesis, which is in line with the findings of gain- and loss-of-function experiments in EGFR transgenic mice.[16] Moreover, EGFR appears to play a role in MPNST progression, and its expression is correlated with worse prognostic variables and course.[17]

We investigated the PDGFRA, PDGFRB, and EGFR status through a comprehensive immunohistochemical, biochemical, cytogenetic, and mutational analysis along with the detection of receptor cognate ligands in a consecutive series of 16 NF1-related and 11 sporadic MPNSTs for which formalin-fixed paraffin-embedded (FFPE) and frozen surgical material was available. Additionally, the activation of the RTK downstream pathways was also studied by means of AKT, ERK, and mTOR Western blotting (WB) experiments, as well as *RAS*, *BRAF*, *PI3KCA*, and *PTEN* mutational analysis and fluorescence in situ hybridization (FISH).

The results indicate that both NF1-related and sporadic MPNSTs show PDGFRA, PDGFRB, and EGFR upstream activation, as well as the activation of RTK downstream signaling, possibly this latter sustained by different mechanisms in the two groups. These findings suggest that a combined RTK and mTOR drug inhibition should have efficacy in the treatment of MPNST.

Materials and Methods

Samples and Patients

We analyzed 27 surgical specimens taken from 25 patients diagnosed as having MPNST at Fondazione IRCCS Istituto Nazionale dei Tumori between 1989 and 2000: 14 had NF1 with an associated MPNST, and 11 were classified as having sporadic tumors because they had no clinical signs or family history of NF1, as previously described.[8]

The samples had been previously characterized in terms of *TP53* alterations[4] and $p15^{INK4b}$, $p14^{ARF}$, and $p16^{INK4a}$ inactivation.[8]

Immunohistochemistry

The immunohistochemistry (IHC) analyses were made on 2-μm cut from FFPE tumoral sections, which were treated with 3% H_2O_2 and then underwent antigen retrieval using 5 mM citrate buffer (pH 6) or 1 mM EDTA (pH 8) in an autoclave at 95°C for 6–15 min. We used antibodies against PDGFRA (clone sc338, Santa Cruz Biotechnology, Santa Cruz, CA, USA; 1:200) and PDGFRB (clone sc339, Santa Cruz Biotechnology; 1:100). All staining was carried out using primary antibody enhancer and polymer following the supplier's protocol (UltraVision LP Large Volume Detection System, horseradish peroxidase [HRP] polymer; Lab Vision, Fremont, CA, USA) and developed using the liquid diaminobenzidine (DAB)-positive substrate chromogen system (Dako, Glostrup, Denmark). The cutoff for positive evaluation was >50% of cells showing cytoplasmic moderate/strong immunolabeling. A gastrointestinal stromal tumor (GIST) carrying the PDGFRA exon 18 mutation was used as a positive control for the PDGFRA staining,[18] and a chordoma was used as a positive control for PDGFRB reactivity.[19]

EGFR was immunostained using the Dako EGFR pharmDx kit, and the level of staining was scored as high, intermediate, and low as previously described.[20]

Biochemical Analyses

Proteins were extracted from frozen tissue[21] and examined by means of PDGFRA and PDGFRB immunoprecipitation (IP) and WB.[22] After EGFR IP using monoclonal EGFR antibody (528:sc-120, Santa Cruz Biotechnology), the filters were incubated with antiphosphotyrosine mouse monoclonal antibody (clone 4G10, Upstate, Lake Placid, NY, USA; 1:4,000) and then with EGFR antibody (1005:sc-03, Santa Cruz Biotechnology; 1:200).

For the PTEN WB experiments, 20 μg of cytoplasmic total protein extract was used with PTEN polyclonal antibody (9552, Cell Signaling Technology, Danvers, MA, USA; 1:1,000). For the AKT, ERK, and mTOR WB experiments, protein extracts were used with the anti-phosphorylated (phospho)-Akt Ser 473 polyclonal antibody (9271, Cell Signaling), anti-phospho-ERK monoclonal antibody (4376, Cell Signaling), or anti-phospho-mTOR antibody (2971, Cell Signaling), diluted 1:1,000. Subsequently, the filters were stripped and incubated with anti-Akt polyclonal antibody (9272, Cell Signaling), anti-ERK polyclonal antibody (9102, Cell Signaling), or anti-mTOR antibody (2972, Cell Signaling), diluted 1:1,000.

As positive controls of expression/phosphorylation, we used the NIH3T3 cell line (American Type Culture Collection, Manassas, VA, USA) for PDGFRA; the Cal27 cell line for EGFR; the 2N5A cell line (derived from the NIH3T3 cell line and expressing the collagene type 1 (COL1)-PDGFB fusion characterizing dermatofibrosarcoma protuberans, kindly provided by Dr. A. Greco, Experimental Oncology Department, Fondazione IRCCS Istituto Nazionale dei Tumori, Milan, Italy) for PDGFRB, AKT, and ERK1/2; and the A431 cell line for PTEN and mTOR.

Fluorescence In Situ Hybridization

The *PDGFRA* and *PDGFRB* FISH analyses were made on 2-μm sections cut from FFPE samples using bacterial artificial chromosome (BAC) clones RP11-231C18 (*PDGFRA* gene, 4q12) and RP11-368019 (*PDGFRB* gene, 5q31-32) as FISH probes, and Spectrum Orange-labeled CEP 4 (Vysis, Downers Grove, IL, USA) and BAC clone RP1152C13 (chromosome 5p11.1) as control probes.[22] The *EGFR* analysis was made using the LSI EGFR/CEP 7 Dual-Color Probe (32-191053 Vysis) as previously described;[8] the PI3KCA analysis using BAC RP11-466H15 (*PI3KCA* gene, 3q26.3) and Spectrum Orange labeled-CEP 3 (Vysis); and the PTEN analysis using the LSI PTEN SO/CEP 10 SG Dual-Color Probe (Vysis).

Mutational Analysis

After DNA extraction from frozen tissue,[8] mutations were analyzed on genomic DNA: all of the PCR products underwent automated DNA sequencing (3100 ABI-PRISM Genetic Analyzer, Applied Biosystems, Foster City, CA, USA), and each sequence reaction was performed at least twice.

PDGFRA. Exons 10, 12, and 18 were amplified using the following primer sequences and annealing temperatures: exon 10, forward 5'-GACTCTCAGGAATTGGCC-3', reverse 5'-CAGCTGATGAGTTGTCCTG-3', annealing temperature 58°C; exon 12, forward 5'-GAACGTTGTTGGACTCTACTGTG-3', reverse 5'-GCAAGGGAAAAGGGAGTCT-3', annealing temperature 60°C; and exon 18, forward 5'-CTTGCAGGGGTGATGCTAT-3', reverse 5'-AGAAGCAACACCTGACTTTAGAGATTA-3', annealing temperature 65°C. The primers and PCR conditions used to amplify exon 14 have been previously described.[23]

PDGFRB. Exons 10, 12, 14, and 18 of the *PDGFRB* gene were amplified.[24]

EGFR. Exons 18, 19, 20, and 21 of the *EGFR* gene were amplified.[25]

K-, H-, and N-*RAS*. Exons 1 and 2 were amplified using the following primer sequences: K-*RAS* exon 1, forward 5'-TGGTGGAGTATTTGATAGTGT-3', reverse 5'-CATGAAAATGGTCAGAGA-3'; K-*RAS* exon 2, forward 5'-GGTGCACTGTAATAATCCAGAC-3', reverse 5'-TGATTTAGTATTATTTATGGC-3'; H-*RAS* exon 1, forward 5'-ATGACGGAATATAAGCTGGT-3', reverse 5'-CGCCAGGCTCACCTCTATA-3'; H-*RAS* exon 2, forward 5'-GATTCCTACCGGAAGCAGGTG-3', reverse 5'-CTGTACTGGTGGATGTCCTC-3'; N-*RAS* exon 1, forward 5'-CAGGTTCTTGCTGGTGTGAA-3', reverse 5'-CACTGGGCCTCACCTCTATG-3'; N-*RAS* exon 2, forward 5'-TTCTTACAGAAAACAAGTGGTTATA-3', reverse 5'-ACCTGTAGAGGTTAATATCCGCAA-3'.

BRAF. Exons 11 and 15 were amplified.[26]

PI3KCA. Exons 9 and 20 of the *PI3KCA* gene were amplified.[27]

PTEN. Exons 5–9 were amplified at an annealing temperature of 55°C using the following primers: exon 5, forward 5'-TGCAACATTTCTAAAGTTACCTACT-3', reverse 5'-GAGGAAAGGAAAAACATCAAAAA-3'; exon 6, forward 5'-TTTTTCAATTTGGCTTCTCTTTTT-3', reverse 5'-TGTTCCAATACATGGAAGGATG-3'; exon 7, forward 5'-CAGTTAAAGGCATTTCCTGTG-3', reverse 5'-TTTTGGATATTTCTCCCAATGAA-3'; exon 8, forward 5'-GTCATTTCATTTCTTTTTCTTTTC-3', reverse 5'-AAGTCAACAACCCCCACAAA-3'; exon 9, forward 5'-TCATGGTGTTTTATCCCTCTTG-3', reverse 5'-TGAGTCATATTTGTGGGTTTTCA-3'.

Ligand Assessment

After RNA extraction and retrotranscription,[8] *PDGFA* and *PDGFB* cDNA were amplified as previously described.[22] Tumor growth factor-α (TGF-α) cDNA was amplified by means of real-time PCR using a TaqMan assay (ABI-PRISM 5700 PCR Sequence Detection Systems, Applied Biosystems). Each reaction was performed using 10 μl of 1× TaqMan Universal Master Mix (Applied Biosystems), 1 μl Assays-on-Demand (Applied Biosystems), consisting of a mix of unlabeled PCR primers and a TaqMan probe (FAM dye-labeled) for the target gene, and 1 μl template cDNA. Cycling was started with 2 min at 50°C and 10 min at 95°C, followed by 40 cycles of 15 s at 95°C and 1 min at 60°C. All of the experiments were performed in triplicate. Glyceraldehyde 3-phosphate dehydrogenase (*GAPDH*) mRNA, detected by a specific probe, was used as an internal control. The $2^{-\Delta\Delta Ct}$ method was used.

Statistical Analysis

Fisher's two-tailed exact test was used to calculate *p*-values, and the level of significance was set at $P = 0.05$.

Results

RTK Upstream Analysis

Immunohistochemistry. The IHC analyses of 16 NF1-related and 10 sporadic MPNSTs revealed the following PDGFRA, PDGFRB, and EGFR expression profiles.

PDGFRA. Cytoplasmic immunoreactivity was present in all of the NF1-related MPNSTs (Table 1) and sporadic MPNSTs (Table 2). PDGFRA staining was more intense than in the GIST-positive control in four MPNSTs and less intense in the NF1-related case 13. Sporadic case 7 showed diffuse cytoplasmic positivity with perinuclear "dotlike" staining, which correlates with *PDGFRA* mutation in GISTs;[28] however, mutational analysis showed a wild-type genotype (see below).

PDGFRB. All but one of the MPNSTs were positive for PDGFRB immunoreactivity (Tables 1 and 2). The staining was cytoplasmic and similar to that observed in the chordoma positive control, except for NF1-related case 6a, which showed more intense PDGFRB staining.

EGFR. EGFR immunoreactivity was more frequent in the NF1-related tumors (15 of 16, 93%; Table 1) than in the sporadic cases (6 of 9, 67%; Table 2), but the majority of cases in both groups showed intermediate-high expression.

Biochemical Analysis

The samples with sufficient frozen material (eight NF1-related and eight sporadic cases) were analyzed by means of IP and WB experiments to assess PDGFRA, PDGFRB, and EGFR expression and status. The details of these analyses are described in the legend of Fig. 1.

PDGFRA* and *PDGFRB. All of the samples showed PDGFRA and PDGFRB expression with levels of intensity that were similar to or less than those observed in the related positive controls; PDGFRA and PDGFRB phosphorylation levels were similar to or less intense than those in the controls in, respectively, 100% and 87% of cases (Tables 1 and 2). Fig. 1, A and B, shows some representative cases.

EGFR. All of the samples showed EGFR expression and phosphorylation levels that were generally similar to or more intense than those observed in the cell line used as a positive control (Tables 1 and 2). Fig. 1C shows some representative cases.

FISH Analyses

As alterations in gene copy number due to amplification or polysomy may be one of the mechanisms responsible for receptor expression/activation, gene status was assessed by means of FISH.

PDGFRA. Eight cases (35%) showed *PDGFRA* gene amplification and/or polysomy for chromosome 4, where the *PDGFRA* gene is located (Fig. 1D). The NF1-related and sporadic cases shared a similar increase in *PDGFRA* gene copy numbers (36% vs. 33%; Tables 1 and 2).

PDGFRB. Polysomy for chromosome 5 (where *PDGFRB* is located) was found in 6 of 23 cases (26%; Fig. 1E), one of which also showed gene amplification. The NF1-related and sporadic cases shared a similar increase in *PDGFRB* gene copy numbers (21% vs. 33%; Tables 1 and 2).

EGFR. EGFR gene amplification and/or polysomy for chromosome 7 was observed in 14 of 23 cases (61%; Fig. 1F). The NF1-related cases more frequently showed an increase in *EGFR* gene copy number (71%) compared with the sporadic cases (44%), but the difference was not statistically significant (Tables 1 and 2).

***PDGFRA, PDGFRB,* and *EGFR* along with *p16^{INK4a}*.** Cumulatively, the FISH analyses revealed increased copy numbers of the RTK genes (mainly *EGFR*) in 14 of 23 MPNSTs (61%), of which six showed an increased gene copy number of *EGFR*, two increased gene copy numbers of *PDGFRA* and *EGFR*, and six increased gene copy numbers of *PDGFRA*, *PDGFRB*, and *EGFR*.

In order to verify the association between *EGFR* amplification and *p16^{INK4a}* gene deletion reported by Perry et al.,[15] we correlated the previously analyzed *p16^{INK4a}* gene status of our samples with their RTK gene status.[8] Eight of the 14 cases (57%) with increased copy numbers of RTK genes also showed *p16^{INK4a}* inactivation due to homozygous deletion or promoter methylation (Tables 1 and 2). However, the association between *p16^{INK4a}* inactivation and the gain in RTK gene copy numbers was not statistically significant.

Mutational Analysis

To verify the mechanism of the RTK activation observed in the IP/WB experiments, we also investigated the presence of RTK gain-of-function mutations.

PDGFRA. The extracellular region (exon 10), juxtamembrane region (exon 12), and tyrosine kinase domain (exons 14 and 18) were automatically sequenced, and all of the samples showed a wild-type *PDGFRA* gene (Tables 1 and 2).

PDGFRB. *PDGFRB* gene sequencing did not reveal any activating mutations, but we observed the silent mutation Leu587Leu (CTG→CTA) in sporadic case 1, and the polymorphism Glu485Lys (GAG→AAG) in three cases.[24]

EGFR. No activating mutations were observed in the *EGFR* gene, but in sporadic MPNSTs, we found two silent mutations in exon 20: Gln787Gln (CAA→CAG) and Thr783Thr (ACC→ACT) (Table 2).

Table 1. RTK analysis of NF1-related MPNSTs

	Protein Analysis									DNA Analysis						Ligands		
	PDGFRA			PDGFRB			EGFR			PDGFRA		PDGFRB		EGFR				
Case	IHC	WB Exp	WB P	IHC	WB Exp	WB P	IHC	WB Exp	WB P	FISH	Mut	FISH	Mut	FISH	Mut	PDGFA	PDGFB	TGF-α
1a	pos	NE	NE	pos	NE	NE	High	NE	NE	D	NE	D	NE	**A**	NE	+	+	+
1b[b]	pos	+	+	pos	+	++	High	++	++	D	wt	T	wt	**LP**	wt	+	+	+
2[b]	pos	+	-	pos	+++	++	Intermediate	NE	NE	**A**	wt	**HP**	wt	**LP**	wt	+	+	+
3b	pos	NE	NE	pos	NE	NE	High	NE	NE	D	wt	T	wt	T	wt	NE	NE	NE
4	pos	NE	NE	pos	NE	NE	High	NE	NE	D	wt	D	Glu485Lys[a]	**A**	wt	NE	NE	NE
5[b]	pos	NE	NE	pos	+	+	High	+++	+++	**HP**	wt	T	wt	**HP**	wt	NE	NE	NE
6a	High	+	+	High	+	+	Low	+	+	**LP**	wt	**HP**	wt	**HP**	wt	+	+	+
6c[c]	High	NE	NE	pos	NE	NE	Intermediate	NE	NE	**LP**	wt	**HP**	wt	**HP**	wt	NE	NE	NE
7	pos	++	++	pos	++	++	High	++	++	**LP**	wt	T	nv	**HP**	wt	+	+	+
8[b]	pos	+	+	pos	NE	NE	Low	+++	+++	D	wt	D	wt	**LP**	wt	+	+	+
9	pos	NE	NE	pos	NE	NE	neg	NE	NE	D	wt	D	NE	D	wt	NE	NE	NE
10	pos	++	++	pos	++	++	High	+++	+++	D	wt	T	Glu485Lys[a]	**LP**	wt	+	+	+
11	pos	NE	NE	pos	NE	NE	High	NE	NE	D	wt	D	wt	D	wt	+	+	+
12	pos	NE	NE	pos	NE	NE	Intermediate	NE	NE	D	wt	T	wt	D	wt	+	+	+
13	Low	++	++	neg	+	++	High	++	++	NE	NE	NE	NE	NE	NE	+	+	+
14	pos	NE	NE	pos	NE	NE	Low	NE	NE	NE	wt	NE	wt	NE	wt	+	+	+

Abbreviations: IHC, immunohistochemistry; WB Exp, receptor expression by Western blot; WB P, receptor phosphorylation by Western blot; FISH, fluorescence in situ hybridization; Mut, mutational status of receptors; PDGFRA, platelet-derived growth factor receptor A; PDGFRB, platelet-derived growth factor receptor B; TGF-α, transforming growth factor-a; pos, positive; neg, negative; +, level lower than in the positive control; ++, level similar to that in the positive control; +++, level higher than in the positive control; D, disomy; A, gene amplification; LP, low polysomy; HP, high polysomy; T, trisomy; NE, not evaluable; wt, wild type.

[a] Polymorphism.

[b] Cases carrying *p16* homozygous deletions.

[c] Case carrying *p16* promoter methylation.

Table 2. RTK analysis of sporadic MPNSTs

	Protein Analysis									DNA Analysis						Ligands		
	PDGFRA			PDGFRB			EGFR			PDGFRA		PDGFRB		EGFR				
Case	IHC	WB Exp	WB P	IHC	WB Exp	WB P	IHC	WB Exp	WB P	FISH	Mut	FISH	Mut	FISH	Mut	PDGFA	PDGFB	TGF-α
1[d]	pos	+	+	pos	+	+	neg	NE	NE	D	wt	D	Leu787Leu[a]	D	wt	+	+	+
2[e]	High	+++	++	pos	++	+	High	++	++	**A**	wt	**HP**	wt	**HP**	wt	-	+	+
3	NE	+	-	NE	+	+	NE	+	+	D	wt	D	wt	D	wt	+	+	+
4	pos	NE	NE	pos	NE	NE	High	NE	NE	NE	wt	NE	wt	NE	Gln787Gln[a]	+	+	+
5[d]	pos	++	+	pos	+	++	neg	NE	NE	T	wt	D	wt	**LP**	wt	-	+	+
6	pos	++	++	pos	++	+	High	NE	NE	D	wt	T	wt	T	wt	NE	NE	NE
7	Dotlike	++	++	pos	+	+	NE	+	+	**LP**	wt	**LP**	wt	**HP**	wt	+	+	+
8	High	NE	NE	pos	NE	NE	neg	NE	NE	NE	wt	NE	Glu485Lys[b]	NE	wt	+	+	-
9[d]	pos	NE	NE	pos	NE	NE	High	NE	NE	**LP**	wt	**A**	wt	**A**	wt	+	+	+
11[d]	pos	+	+	pos	+	+	Low	+	+	D	wt	D	wt	D	Thr783Thr[a]	NE	NE	NE
12	pos	+	++	pos	+	++	Intermediate	+++	++	D	wt	D	wt	D	wt	+	-[c]	-[c]

Abbreviations: PDGFRA, platelet-derived growth factor receptor A; IHC, immunohistochemistry; WB Exp, receptor expression by Western blot; WB P, receptor phosphorylation by Western blot; PDGFRB, platelet-derived growth factor receptor B; EGFR, epidermal growth factor receptor; FISH, fluorescence in situ hybridization; Mut, mutational status of receptor; TGF-α, transforming growth factor-a; pos, positive; neg, negative; +, level lower than in the positive control; ++, level similar to that in the positive control; +++, level higher than in the positive control; D, disomy; A, gene amplification; LP, low polysomy; HP, high polysomy; T, trisomy; NE, not evaluable; wt, wild type.

[a] Silent mutation.

[b] Polymorphism.

[c] Absent.

[d] Cases carrying *p16* homozygous deletions.

[e] Cases carrying *p16* promoter methylation.

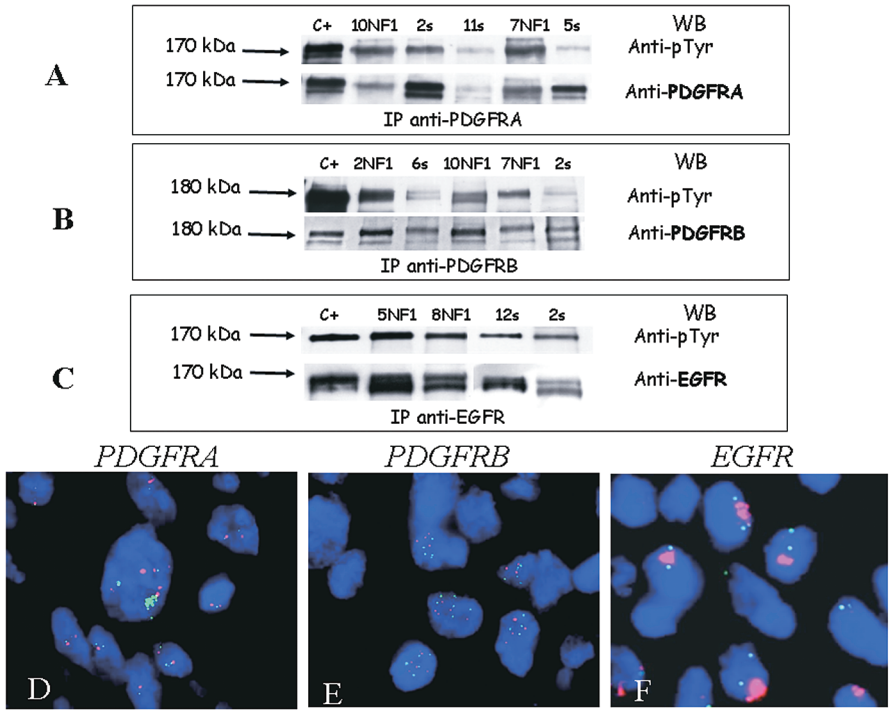

Fig. 1. (A–C) Receptor tyrosine kinase (RTK) biochemical analyses. (A) Platelet-derived growth factor (PDGF) receptor A (PDGFRA) immunoprecipitation (IP) and Western blotting (WB) experiments revealed a 170-kDa band corresponding to the activated (upper arrow) and expressed (lower arrow) receptor in the tumor samples. PDGFRA phosphorylation levels were similar to (cases 10 neurofibromatosis type 1 [NF1], 7 NF1, and 2s) or less intense than (cases 11s and 5s) those found in the positive control (NIH3T3 cell line). pTyr, phosphorylated tyrosine. (B) PDGF receptor B (PDGFRB) IP and WB revealed a 180-kDa band corresponding to activated (upper arrow) and expressed (lower arrow) PDGFRB in all analyzed cases. The samples showed different phosphorylation levels: similar to (NF1-related cases 10 [10NF1] and 7NF1), more intense than (case 2NF1), or less intense than (cases 6s and 2s) those observed in the 2N5A cells used as positive controls. (C) Epidermal growth factor receptor (EGFR) analysis revealed a band of 170 kDa in all of the analyzed samples, thus indicating the presence of activated (upper arrow) and expressed (lower arrow) EGFR. The level of phosphorylation was similar to (cases 12s and 2s) or more intense than (cases 5NF1 and 8NF1) those observed in the positive controls (Cal27 cell line). C+, positive control; s, sporadic case. (D–F) RTK fluorescence in situ hybridization analyses. (D) The nuclei in sporadic case 2 showed *PDGFRA* gene amplification (green cluster) in a high-polysomy chromosome 4 (centromere 4, red signals) where *PDGFRA* is located (green signals). (E) The nuclei in NF1-related case 2 showed a high-polysomy chromosome 5 (centromere 5, red signals) where *PDGFRB* is located (green signals). (F) The nuclei in NF1-related case 1a showed *EGFR* gene amplification (red cluster) in disomy represented by two centromere 7 signals (green signals).

Ligand Expression

To verify whether receptor activation was due to the presence on an autocrine/paracrine loop, we investigated the cognate ligands of each receptor, and found the PDGFA, PDGFB, and TGF-α ligands in 18 out of 20 cases (90%).

All of the NF1-related MPNSTs and 78% of the sporadic MPNSTs expressing the investigated receptors (Tables 1 and 2) coexpressed the corresponding cognate ligands.

EGFR-PDGFRA *and* EGFR-PDGFRB *Heterodimerization*

In three cases, the frozen material was sufficient to investigate a possible presence of EGFR-PDGFRA and EGFR-PDGFRB heterodimers. Protein extracts were immunoprecipitated with EGFR antibody, and then WB experiments were performed using anti-PDGFRA (Fig. 2A) or anti-PDGFRB (Fig. 2B), which revealed the specific bands corresponding to the two PDGF receptors. The further WB using EGFR antibody revealed EGFR expression in all cases. Thus, the results indicated that in MPNST EGFR could transactivate both PDGFRA and PDGFRB through heterodimerization.

Analysis of RTK Downstream Pathways

Biochemical Analysis. The cryopreserved samples investigated for RTK expression/activation were also analyzed for AKT, ERK, and mTOR expression and status by means of WB experiments.

AKT. AKT expression was observed in all of the samples, with the activated form being found in all but one NF1-related MPNST (Table 3) and in all but three sporadic MPNSTs (Table 4). In Fig. 3A some representative cases are reported.

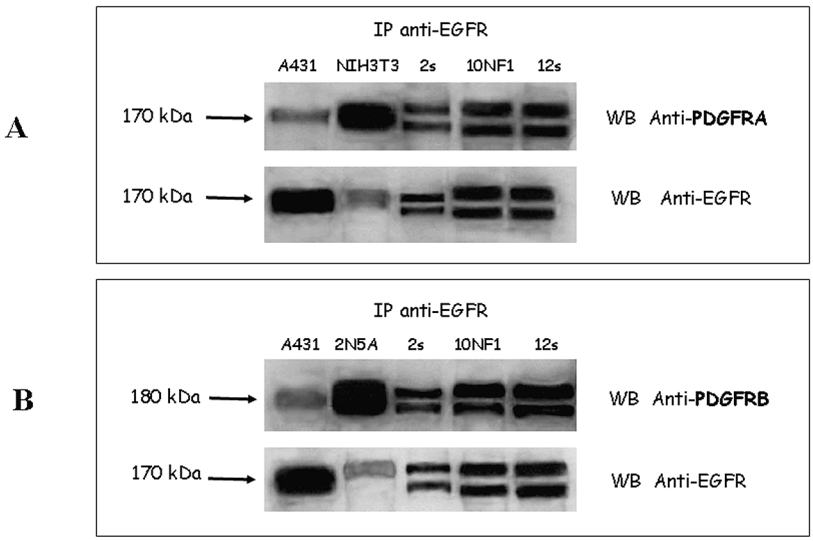

Fig. 2. Epidermal growth factor receptor (EGFR)–platelet-derived growth factor (PDGF) receptor A (PDGFRA) and EGFR–PDGF receptor B (PDGFRB) heterodimerization. (A) EGFR immunoprecipitation (IP) and PDGFRA Western blotting (WB) experiments revealed a 170-kDa band corresponding to PDGFRA showing similar expression in all three analyzed cases (sporadic cases 2 [2s] and 12s and NF1-related case 10 [10NF1]). NIH3T3 cell lines were used as positive control for PDGFRA. Afterward, the filter was stripped and incubated with EGFR antibody, which revealed a band of 170 kDa in all of the analyzed samples, thus indicating less intense expression of EGFR than observed in the positive control A431 cells. (B) EGFR IP and PDGFRB WB experiments revealed a 180-kDa band corresponding to PDGFRB showing similar expression in all three analyzed cases (cases 2s, 10NF1, and 12s). 2N5A cell lines were used as positive control for PDGFRB. Afterward, the filter was stripped and incubated with EGFR antibody, which revealed a band of 170 kDa in all of the analyzed samples, thus indicating the expression of EGFR.

Table 3. Downstream effector analysis of NF1-related MPNSTs

	Biochemical Analysis							DNA Analysis							
	PTEN	AKT		MAPK		mTOR		PI3KCA		PTEN		KRAS	HRAS	NRAS	BRAF
Case	Exp	Exp	Phosph	Exp	Phosph	Exp	Phosph	Mut	FISH	Mut	FISH	Mut	Mut	Mut	Mut
1a	NE	NE	NE	NE	NE	NE	NE	NE	M	NE	D	NE	NE	NE	NE
1b	+	+	-	+	+	-	+	wt	D	wt	D	wt	wt	wt	wt
2	NE	++	+	++	+	NE	NE	wt	D	wt	**M**	wt	wt	wt	wt
3b	NE	NE	NE	NE	NE	NE	NE	wt	D	wt	**M**	wt	wt	wt	wt
4	NE	NE	NE	NE	NE	NE	NE	wt	D	wt	D	wt	wt	wt	wt
5	-	++	+	++	+	+	+	wt	D	wt	D	wt	wt	wt	wt
6a	++	++	+	++	+	+	++	wt	D	wt	**M**	wt	wt	wt	wt
6c	NE	NE	NE	NE	NE	NE	NE	wt	D	wt	D	wt	wt	wt	wt
7	++	++	+	++	+	+	+	NE	NE	NE	LP	NE	NE	NE	NE
8	++	++	+++	++	+	+	+	wt	**LP**	wt	**M**	wt	wt	wt	wt
9	NE	NE	NE	NE	NE	NE	NE	NE	M	NE	**M**	NE	NE	NE	NE
10	++	++	++	++	++	+	++	wt	**LP**	wt	**M**	wt	wt	wt	wt
11	++	NE	NE	NE	NE	NE	NE	wt	NE	wt	D	wt	wt	wt	wt
12	NE	NE	NE	NE	NE	NE	NE	wt	D	wt	D	wt	wt	wt	wt
13	++	++	+	++	+	-	-	NE	NE	NE	NE	NE	NE	NE	NE
14	NE	NE	NE	NE	NE	NE	NE	wt	NE	wt	**NE**	wt	wt	wt	wt

Abbreviations: Mut, mutational status; NE, not evaluable; wt, wild type; FISH, fluorescence in situ hybridization; M, monosomy; D, disomy; LP, low polysomy; Exp, expression; Phosph, phosphorylation; +, level lower than in the positive control; ++, level similar to that in the positive control; -, no expression.

Table 4. Downstream effector analysis of sporadic MPNSTs

	Biochemical Analysis							DNA Analysis							
	PTEN	AKT		MAPK		mTOR		PI3KCA		PTEN		KRAS	HRAS	NRAS	BRAF
Case	Exp	Exp	Phosph	Exp	Phosph	Exp	Phosph	Mut	FISH	Mut	FISH	Mut	Mut	Mut	Mut
1	++	+	-	++	+	NE	NE	wt	D	wt	D	wt	wt	wt	wt
2	++	+	+	++	++	++	++	wt	D	wt	D	wt	wt	wt	wt
3	++	+	-	+	+	+	+	wt	D	wt	D	wt	wt	wt	wt
4	NE	NE	NE	NE	NE	NE	NE	wt	NE	wt	NE	wt	wt	wt	wt
5	++	+	+	++	++	++	++	wt	D	wt	D	wt	wt	Gln61Arg	wt
6	NE	+	+	+	-	NE	NE	wt	D	wt	D	wt	wt	wt	wt
7	++	++	+	++	++	++	+	wt	**LP**	wt	D	wt	wt	wt	wt
8	NE	NE	NE	NE	NE	NE	NE	wt	NE	wt	NE	wt	wt	wt	wt
9	NE	NE	NE	++	+	NE	NE	wt	**LP**	wt	LP	wt	wt	wt	wt
11	++	+	-	++	++	NE	NE	wt	D	wt	D	Gly12Asp	wt	wt	wt
12	++	++	+	NE	NE	++	++	wt	D	wt	D	wt	wt	wt	wt

Abbreviations: Mut, mutational status; NE, not evaluable; wt, wild type; FISH, fluorescence in situ hybridization; D, disomy; LP, low polysomy; Exp, expression; Phosph, phosphorylation; + , level lower than in the positive control; ++, level similar to that in the positive control; -, no expression.

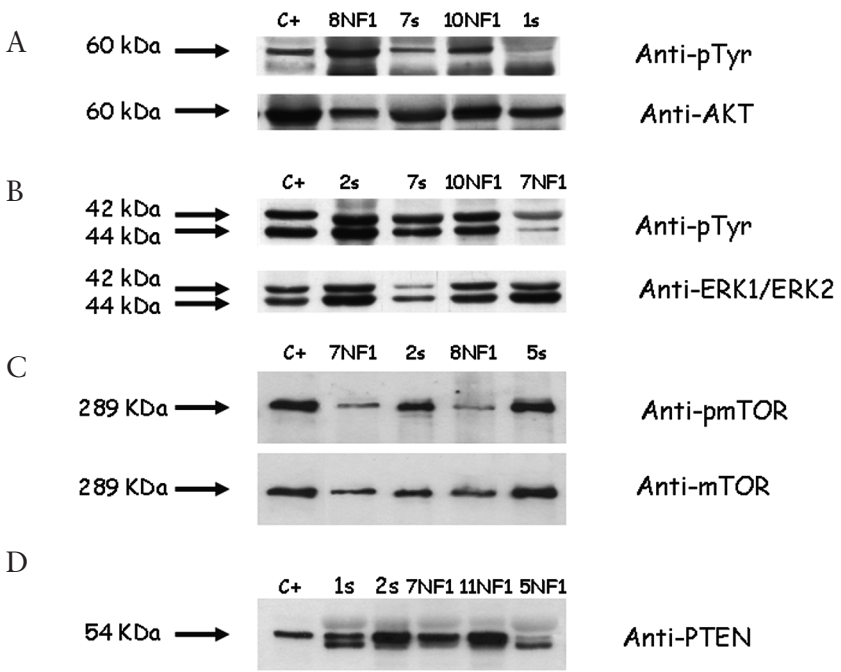

Fig. 3. PTEN, AKT, ERK, and mTOR biochemical analysis. (A) Membrane incubation with phosphorylated Akt Ser 473 and anti-Akt polyclonal antibodies revealed a 60-kDa band corresponding to the activated (upper arrow) and expressed (lower arrow) Akt form. The samples showed phosphorylation levels similar to (NF1-related case 10 [10NF1]) or more (case 8NF1) or less (sporadic cases 7s and 1s) intense than 2N5A cells were used as positive controls. (B) Membrane incubation with both phosphorylated ERK and anti-ERK polyclonal antibodies revealed two bands of 42 and 44 kDa, corresponding to the ERK1 and ERK2 activated (upper arrow) and expressed (lower arrow) forms, respectively. ERK1 and ERK2 phosphorylation levels were similar to (cases 2s, 7s, and 10NF1) or less intense (case 7NF1) than those observed in the 2N5A cells used as positive controls. (C) Membrane incubation with phosphorylated mTOR and anti-mTOR polyclonal antibodies revealed a 289-kDa band corresponding to the activated (upper arrow) and expressed (lower arrow) mTOR form. Phosphorylation levels were similar to (cases 2s and 5s) or less intense (cases 7NF1 and 8NF1) than those observed in A431 cells used as positive control. (D) Membrane incubation with PTEN antibody revealed a 54-kDa band in all cases (cases 1s, 2s, 7NF1, and 11NF1) except in one case (case 5NF1) that showed reduced PTEN expression compared to A431 cell line used as positive control. C+, positive control.

ERK. ERK1 and ERK2 were expressed in all samples at levels generally similar to those observed in the positive control (Tables 3 and 4). In all but one MPNST, membrane incubation with the phospho-ERK polyclonal antibody revealed two bands of 42 and 44 kDa, corresponding to the active forms of ERK1 and ERK2, respectively (Tables 3 and 4). In Fig. 3B some representative cases are reported.

mTOR. mTOR expression was observed in all but two cases (Tables 3 and 4). All but one case (NF1-related case 13) showed mTOR phosphorylation at a level that was lower than or similar to that observed in the positive control. In Fig. 3C some representative cases are reported.

PI3KCA *and* PTEN *Analysis*

Mutational analysis. No mutations were found after the DNA sequencing of exons 9 and 20 of *PI3KCA*, and exons 5–9 of *PTEN* (Tables 3 and 4).

FISH. A normal disomic *PI3KCA* pattern was found in 15 out of 21 cases (71%: 67% of the NF1-related tumors and 78% of the sporadic tumors); 19% of the samples (17% NF1-related and 22% sporadic) showed low polysomy of chromosome 3, where *PI3KCA* gene is located, and two NF1-related MPNSTs (17%) were monosomic (Tables 3 and 4).

Fifty percent of the NF1-related MPNSTs showed a decrease in the *PTEN* gene copy number consisting of monosomy of chromosome 10 ($p = 0.018$) (Table 3); the sporadic cases generally had a normal disomic pattern (89%) (Table 4).

To verify if the gene status yielded changes of PTEN expression, PTEN was investigated by means of WB experiments. One sample showed no PTEN expression (NF1-related case 5), which was reduced in another (NF1-related case 1b); in the remaining cases, PTEN expression was similar to that observed in the positive control (Tables 1 and 2). Fig. 3D shows some representative cases.

RAS *and* BRAF *Mutational Analysis*

No K-, H-, or N-*RAS* mutations were found in 12 NF1-related tumors (Table 3), whereas 2 of 11 sporadic cases (18%) were mutated (Table 4): case 11 showed the K-*RAS* mutation Gly12Asp (GGT→GAC) and case 5 the N-*RAS* mutation Gln61Arg (CAA→CGA). The same samples were further investigated for *BRAF* gene mutations, but none was found (Tables 3 and 4).

Discussion

The aim of this study was to explore the biochemical/cytogenetic/molecular bases of activation of PDGFRA, PDGFRB, and EGFR and their downstream pathways as potential therapeutic targets in a series of consecutive NF1-related and sporadic MPNSTs for which cryopreserved and formalin-fixed surgical material was available. The results confirm and extend previously reported preclinical biochemical findings and immunohistochemical and mutational analysis data collected in a clinical setting, suggesting that PDGFRA and PDGFRB should be considered candidates for targeted therapy with imatinib,[11,13] and add the suggestion of considering combined RTK and mTOR inhibitor treatments for both NF1-related and sporadic MPNSTs.

Regarding RTK, our biochemical findings showed that all of the MPNSTs had PDGFRA, PDGFRB, and EGFR activation. In particular, both in sporadic and in NF1-related MPNSTs, PDGFRA and PDGFRB expression/phosphorylation levels were similar to or lower than those observed in the related positive controls, and the same was true for EGFR in sporadic cases. On the contrary, the NF1-related tumors had higher levels of EGFR expression/phosphorylation compared with the positive control. Although not entirely superimposable, the immunoexpression data and the FISH analysis followed a similar trend, the latter indicating a more frequent occurrence of increased *EGFR* gene copy numbers among the NF1-related tumors (10 of 14 cases). Because a gain in gene copy number may be responsible for RTK expression/activation, it is not surprising that the FISH results were roughly consistent with the biochemical analyses. Interestingly, the gain in *EGFR* in half of the NF1-related MPNSTs and all of the sporadic cases paralleled the gain in both *PDGFRA* and *PDGFRB* (six cases) or *PDGFRA* alone (two cases). We have previously reported that 8 of the 14 cases harboring a gain in RTK gene copy number also showed p16 inactivation mainly due to homozygous deletions,[8] and it seems that MPNSTs are characterized by a high degree of genetic instability, particularly the syndromic cases. However, unlike Perry et al.,[15] who found an association between *EGFR* amplification and $p16^{INK4a}$ homozygous deletions, we did not find that the gains in *EGFR, PDGFRA*, and *PDGFRB* gene copy number segregated with $p16^{INK4a}$ gene loss. Further evidence of the genetic instability of MPNSTs includes the previously described *KIT* gene amplification in NF1-related cases, [11] which we did not investigate in this study because none of the MPNSTs showed KIT expression/activation (data not shown), and our aim was to verify the potential role of RTKs as drug targets.

The sequencing of *PDGFRA*, *PDGFRB*, and *EGFR* genes from the transmembrane domain to the COOH terminus did not reveal any activating point mutations in our series. This is in line with the literature, which reported occasional PDGFRA mutations[11] and no EGFR somatic mutations[29] in MPNST. Furthermore, the presence of the cognate ligands PDGFA, PDGFB, and TGF-α in 90% of the cases strongly supports the idea that receptor activation is sustained by an autocrine loop.[29]

In addition to ligand-dependent mechanism, we demonstrated that heterodimerization-mediated crosstalk between EGFR and PDGFR families may concur to RTK activation. This activation profile is in line with the recently stressed combined treatments aimed to inhibit multiple activated RTKs in the presence of tumors carrying coactivated RTK profiles.[30]

However, recent findings pointing out that K-*RAS*/*BRAF* activation,[31,32] *PI3KCA* activation,[33] or the loss of PTEN expression,[34] leading to AKT and mitogen-activated protein kinase activation, may be significantly associated with a nonresponse to anti-EGFR treatments prompted us to extend our analyses to RTK downstream signaling. Indeed, IP/WB experiments showed expression and phosphorylation of AKT, ERK, and mTOR in both NF1-related and sporadic cases. Moreover, no activating *BRAF* or *PI3KCA* mutations, nor any inactivating *PTEN* mutations,[35] were detected in either group of MPNSTs; however, we found mutations of RAS family genes in 18% of the sporadic MPNSTs, and *PTEN* gene monosomy restricted to 50% of the NF1-related cases ($p = 0.018$). Given the essential role played by PTEN in maintaining chromosomal stability by means of physical interactions with centromeres,[36] this last finding may explain the greater degree of genetic instability found in the NF1-related cases. Interestingly, regardless of *PTEN* gene status, no changes in PTEN expression were observed in any of the MPNSTs with respect to the positive control (A431 cell line), except for two non-mutated and disomic NF1-related cases in which PTEN expression was reduced or absent; this finding suggests that *PTEN* monosomy seems neutral for its effect on PTEN expression. However, it was not possible to compare PTEN expression between tumor and normal tissue in each case due to the lack of frozen normal tissue. This comparison would be advisable because a possible reduced PTEN expression in tumor samples carrying *PTEN* monosomy may be consistent with PTEN functional haploinsufficiency,[37] potentially critical for tumor progression and response to RTK inhibitors. We also observed the similar occurrence of an increased *PI3KCA* gene copy number in both the sporadic and NF1-related cases (22% vs. 17%), but its functional role is not clear. Thus, through this upstream and downstream RTK signaling analysis, we observed, in addition to the activation of upstream RTKs, the expression and phosphorylation of downstream kinase family such as AKT, ERK, and mTOR in both sporadic and NF1-related cases, possibly sustained by two different mechanisms. Indeed, in all but two sporadic MPNSTs the activation of downstream signaling seems to be driven by both ligand-dependent and heterodimerization-dependent upstream RTK activation, since no alterations of upstream mTOR effectors were observed and the presence of cognate ligands, along with EGFR/PDGFRA and EGFR/PDGFRB heterodimers, was demonstrated. On the contrary, in the two RAS-mutated sporadic cases and, by definition, the NF1-related cases, the activation of ERK/mTOR seems to be mainly mediated by *RAS* mutation and by RAS activation through *NF1* germline deletion/neurofibromin loss, respectively.

In conclusion, these findings might open up a new avenue for the development of kinase inhibitor treatments in MPNST, strongly suggesting that, irrespectively to the underlined mechanism, a combination treatment targeting RTKs and mTOR might be more effective than targeting the receptor alone. Consistently, erlotinib treatment does not seem to show efficacy in metastatic unresectable sporadic and NF1-related MPNST patients in a phase II trial,[38] while at preclinical level a significant additional inhibitory effect of growth on MPNST xenografts has been achieved applying an anti-EGFR and mTOR combined therapy.[39] Further clinical trials are strongly hoped.

Acknowledgments

We gratefully acknowledge the contribution of Dr. Milo Frattini to the *BRAF* mutational analysis. This work was supported by Associazione Italiana per la Ricerca sul Cancro grants.

References

1. Anghileri M, Miceli R, Fiore M, et al. Malignant peripheral nerve sheath tumors: prognostic factors and survival in a series of patients treated at a single institution. *Cancer*. 2006;107:1065–1074.
2. Holtkamp N, Atallah I, Okuducu AF, et al. MMP-13 and p53 in the progression of malignant peripheral nerve sheath tumors. *Neoplasia*. 2007;9:671–677.
3. Menon AG, Anderson KM, Riccardi VM, et al. Chromosome 17p deletions and p53 gene mutations associated with the formation of malignant neurofibromatosis. *Proc Natl Acad Sci USA*. 1990;87:5435–5439.
4. Birindelli S, Perrone F, Oggionni M, et al. Rb and TP53 pathway alterations in sporadic and NF1-related malignant peripheral nerve sheath tumors. *Lab Invest*. 2001;81:833–844.
5. Legius E, Dierick H, Wu R, et al. TP53 mutations are frequent in malignant NF1 tumors. *Genes Chromosomes Cancer*. 1994;10:250–255.
6. Upadhyaya M, Kluwe L, Spurlock G, et al. Germline and somatic NF1 gene mutation spectrum in NF1-associated malignant peripheral nerve sheath tumors (MPNSTs). *Hum Mutat*. 2008;29:74–82.
7. Koga T, Iwasaki H, Ishiguro M, Matsuzaki A, Kikuchi M. Frequent genomic imbalances in chromosomes 17, 19, and 22q in peripheral nerve sheath tumours detected by comparative genomic hybridization analysis. *J Pathol*. 2002;197:98–107.
8. Perrone F, Tabano S, Colombo F, et al. p15INK4b, p14ARF, and p16INK4a inactivation in sporadic and neurofibromatosis type 1-related malignant peripheral nerve sheath tumors. *Clin Cancer Res*. 2003;9:4132–4138.
9. Nielsen GP, Stemmer-Rachaminov AO, Ino Y, Moller MB, Rosenberg AE, Louis N. Malignant transformation of neurofibromas in neurofibromatosis 1 is associated with *CDKN2A/P16* inactivation. *Am J Pathol*. 1999;155:1879–1884.
10. Kourea HP, Orlow I, Scheithauer BW, Cordon-Cardon C, Woodruff JM. Deletions of the *INK4A* gene occur in malignant peripheral nerve sheath tumors but not in neurofibromas. *Am J Pathol*. 1999;155:1855–1860.
11. Holtkamp N, Okuducu AF, Mucha J, et al. Mutation and expression of PDGFRA and KIT in malignant peripheral nerve sheath tumors, and

its implications for imatinib sensitivity. *Carcinogenesis*. 2006;27:664–671.

12. Basu TN, Gutmenn DH, Fletcher JA, Glover TW, Collins FS, Downward J. Aberrant regulation of ras proteins in malignant tumour cells from type 1 neurofibromatosis patients. *Nature*. 1992;356:713–715.
13. Aoki M, Nabeshima K, Koga K, et al. Imatinib mesylate inhibits cell invasion of malignant peripheral nerve sheath tumor induced by platelet-derived growth factor-BB. *Lab Invest*. 2007;87:767–779.
14. Declue JE, Heffelfinger S, Benvenuto G, et al. Epidermal growth factor receptor expression in neurofibromatosis type 1-related tumors and NF1 animal models. *J Clin Invest*. 2000;105:1233–1241.
15. Perry A, Kunz SN, Fuller CE, et al. Differential NF1, p16, and EGFR patterns by interphase cytogenetics (FISH) in malignant peripheral nerve sheath tumor (MPNST) and morphologically similar spindle cell neoplasms. *J Neuropathol Exp Neurol*. 2002;61:702–709.
16. Ling BC, Wu J, Miller SJ, et al. Role of epidermal growth factor receptor in neurofibromatosis-related peripheral nerve tumorigenesis. *Cancer Cell*. 2005;7:65–75.
17. Keizman D, Issakov J, Meller I, et al. Expression and significance of EGFR in malignant peripheral nerve sheath tumor [abstract]. *J Clin Oncol*. 2008;26:10588.
18. Perrone F, Tamborini E, Dagrada GP, et al. 9p21 locus analysis in high-risk gastrointestinal stromal tumors characterized for c-kit and platelet-derived growth factor receptor alpha gene alterations. *Cancer*. 2005;104:159–169.
19. Casali P, Messina A, Stacchiotti S, et al. Imatinib mesylate in chordoma. *Cancer*. 2004;101:2086–2097.
20. Perrone F, Suardi S, Pastore E, et al. Molecular and cytogenetic subgroups of oropharyngeal squamous cell carcinoma. *Clin Cancer Res*. 2006;12:6643–6651.
21. Tamborini E, Bonadiman L, Negri T, et al. Detection of overexpressed and phosphorylated wild-type kit receptor in surgical specimens of small cell lung cancer. *Clin Cancer Res*. 2004;10:8214–8219.
22. Lagonigro MS, Tamborini E, Negri T, et al. PDGFRalpha, PDGFRbeta and KIT expression/activation in conventional chondrosarcoma. *J Pathol*. 2006;208:615–623.
23. Lasota J, Stachura J, Miettinen M. GISTs with PDGFRA exon 14 mutations represent a subset of clinically favorable gastric tumors with epithelioid morphology. *Lab Invest*. 2006;86:94–100.
24. Signoroni S, Frattini M, Negri T, et al. Cyclooxygenase-2 and platelet-derived growth factor receptors as potential targets in treating aggressive fibromatosis. *Clin Cancer Res*. 2007;13:5034–5040.
25. Lynch TJ, Bell DW, Sordella R, et al. Activating mutations in the epidermal growth factor receptor underlying responsiveness of non-small-cell lung cancer to gefitinib. *N Engl J Med*. 2004;350:2129–2139.
26. Frattini M, Ferrario C, Bressan P, et al. Alternative mutations of BRAF, RET and NTRK1 are associated with similar but distinct gene expression patterns in papillary thyroid cancer. *Oncogene*. 2004;23:7436–7440.
27. Moroni M, Veronese S, Benvenuti S, et al. Gene copy number for epidermal growth factor receptor (EGFR) and clinical response to anti-EGFR treatment in colorectal cancer: a cohort study. *Lancet Oncol*. 2005;6:279–286.
28. Miselli F, Conca E, Casieri P, et al. A sporadic multiple GIST with unusual pathologic, molecular, and genetic features. *Am J Surg Pathol*. 2008;32:340–341.
29. Holtkamp N, Malzer E, Zietsch J, et al. EGFR and erbB2 in malignant peripheral nerve sheath tumors and implications for targeted therapy. *Neuro-Oncology*. 2008;10(6):946–957.
30. Stommel JM, Kimmelman AC, Nabioullin R, et al. Coactivation of receptor tyrosine kinase affects the response of tumor cells to targeted therapies. *Science*. 2007;318:287–290.
31. Benvenuti S, Sartore-Bianchi A, Dinicolantonio F, et al. Oncogenic activation of the RAS/RAF signaling pathway impairs the response of metastatic colorectal cancers to anti-epidermal growth factor receptor antibody therapies. *Cancer Res*. 2007;67:2643–2648.
32. van Zandwijk N, Mathy A, Boerrigter L, et al. EGFR and KRAS mutations as criteria for treatment with tyrosine kinase inhibitors: retro- and prospective observations in non-small-cell lung cancer. *Ann Oncol*. 2007;18:99–103.
33. Perrone F, Lampis A, Orsenigo M, et al. PI3KCA/PTEN deregulation contributes to impaired responses to cetuximab in metastatic colorectal cancer patients. *Ann Oncol*. 2008;20(1):84–90.
34. Frattini M, Saletti P, Romagnani E, et al. PTEN loss of expression predicts cetuximab efficacy in metastatic colorectal cancer patients. *Br J Cancer*. 2007;97:1139–1145.
35. Mawrin C, Kirches E, Boltze C, Dietzmann K, Roessner A, Schneider-Stock R. Immunohistochemical and molecular analysis of p53, RB, and PTEN in malignant peripheral nerve sheath tumors. *Virchows Arch*. 2002;440:610–615.
36. Shen WH, Balajee AS, Wang J, et al. Essential role for nuclear PTEN in maintaining chromosomal integrity. *Cell*. 2007;128:157–170.
37. Salmena L, Carracedo A, Pandolfi PP. Tenets of PTEN tumor suppression. *Cell*. 2008;133:403–414.
38. Albritton KH, Rankin C, Coffin CM, et al. Phase II study of erlotinib in metastatic or unresectable malignant peripheral nerve sheath tumors (MPNST) [abstract]. *J Clin Oncol*. 2006;24:9518.
39. Johansson G, Mahller YY, Collins MH, et al. Effective in vivo targeting of the mammalian target of rapamycin pathway in malignant peripheral nerve sheath tumors. *Mol Cancer Ther*. 2008;7:1237–1245.